Contents

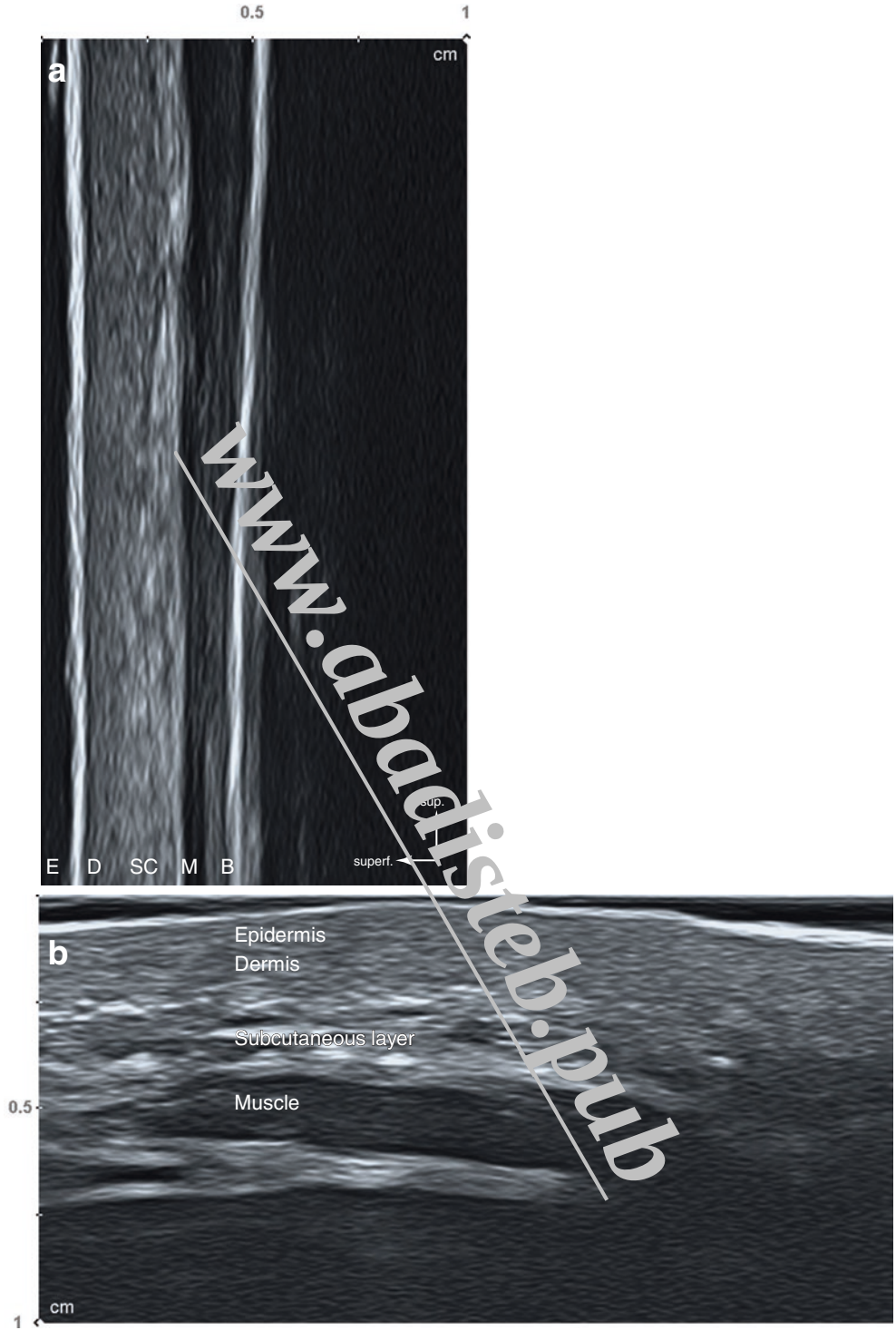

Fig. 2.14 Ultrasonography representing the regional difference of the epidermis (E), dermis (D), subcutaneous tissue (SC), muscle (M), and bone (B). (**a**) Radix (sagittal view, 24 MHz by linear transducer) and (**b**) subzygomatic area (transverse view, 24 MHz by linear transducer). (Published with kind permission of © Hee-Jin Kim 2020. All Rights Reserved)

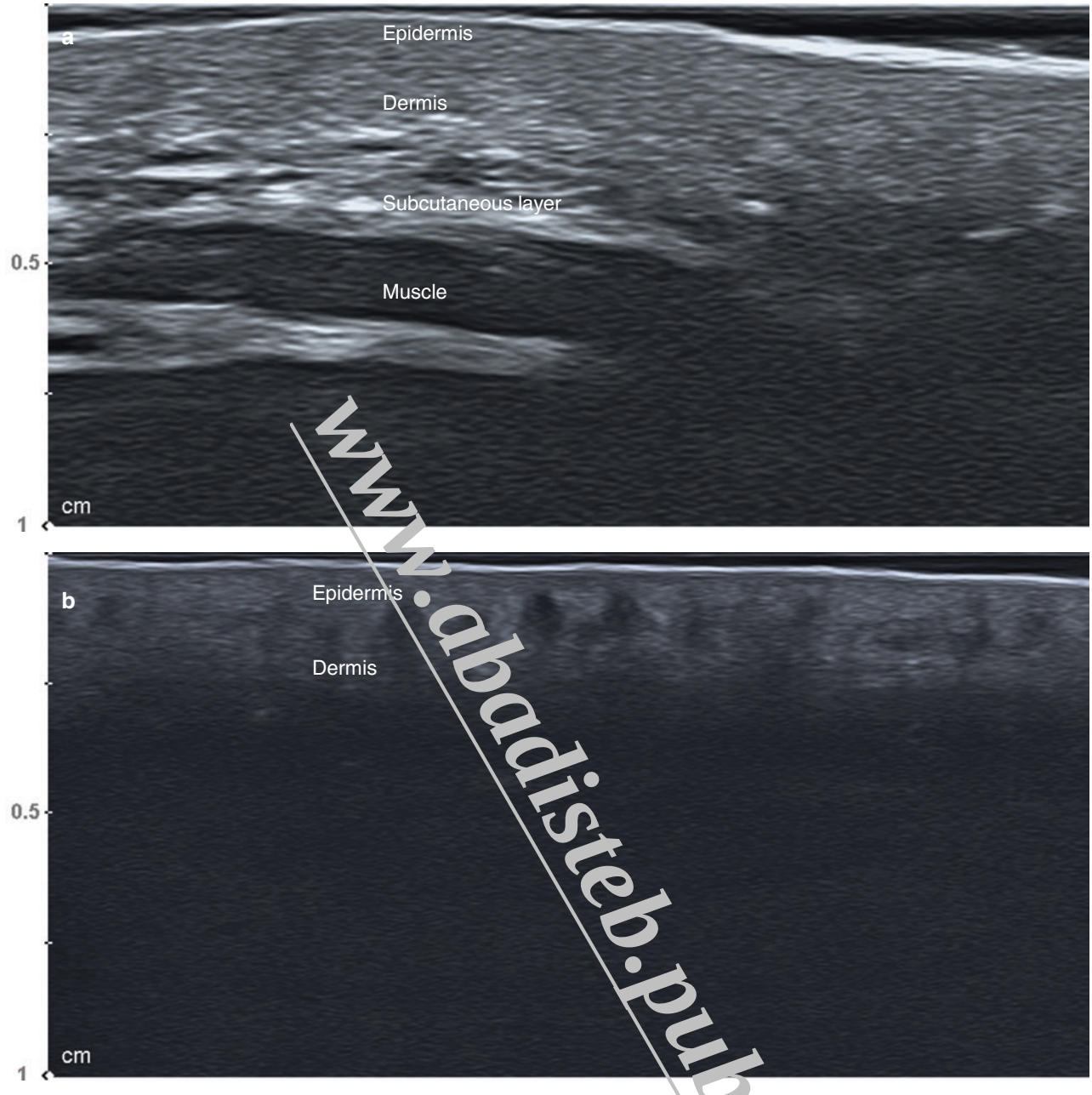

Fig. 2.15 Differences in image resolution of the ultrasonography depending on the frequency. (**a**) 24 MHz by linear transducer (subzygomatic area, transverse view) and (**b**) 32 MHz by linear transducer (subzygomatic area, transverse view). (Published with kind permission of © Hee-Jin Kim 2020. All Rights Reserved)

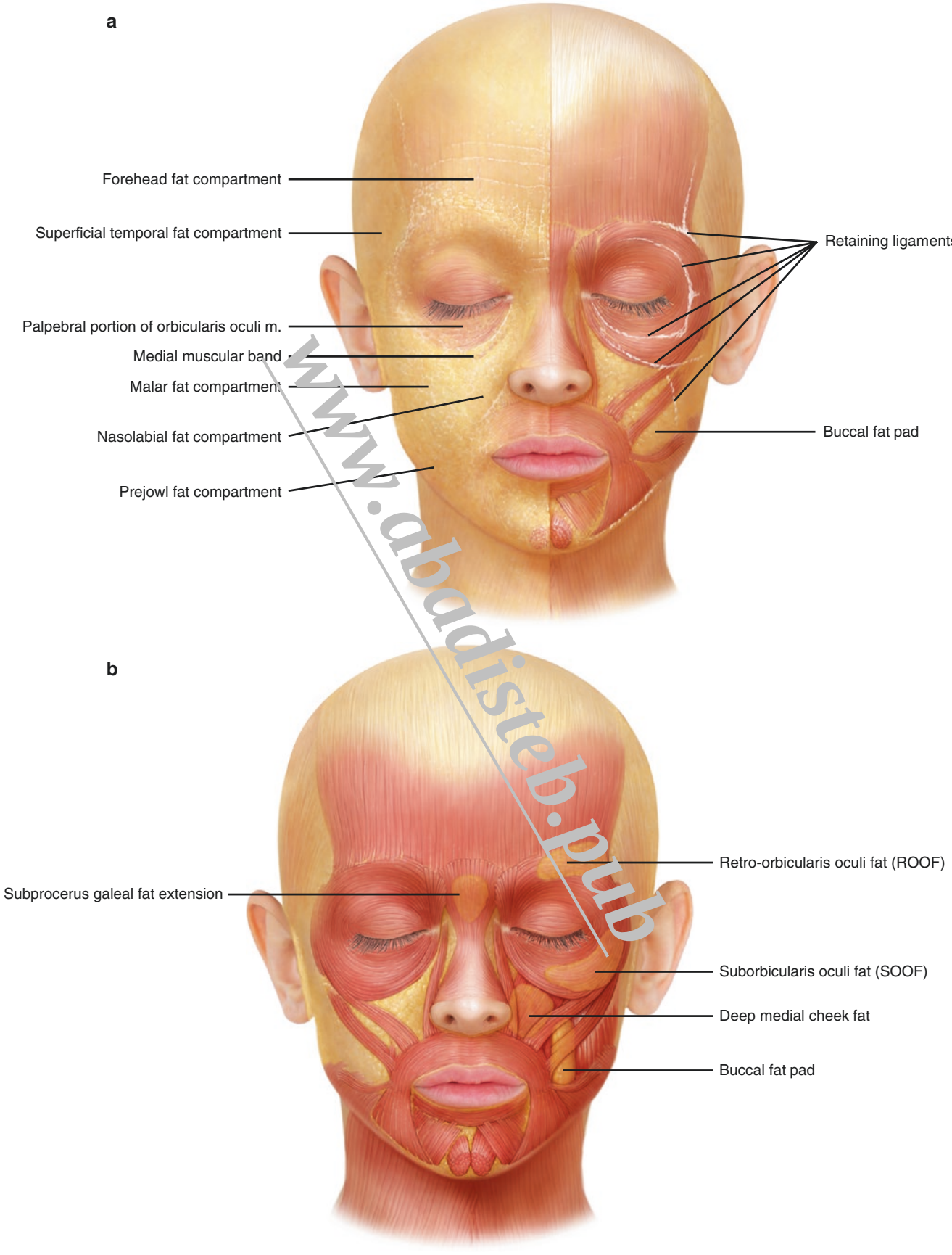

Fig. 2.16 Facial fat compartments. (**a**) Subcutaneous fat and superficial muscles of the face and (**b**) deep fat compartments of the face. (Published with kind permission of © Kwan-Hyun Youn 2020. All Rights Reserved)

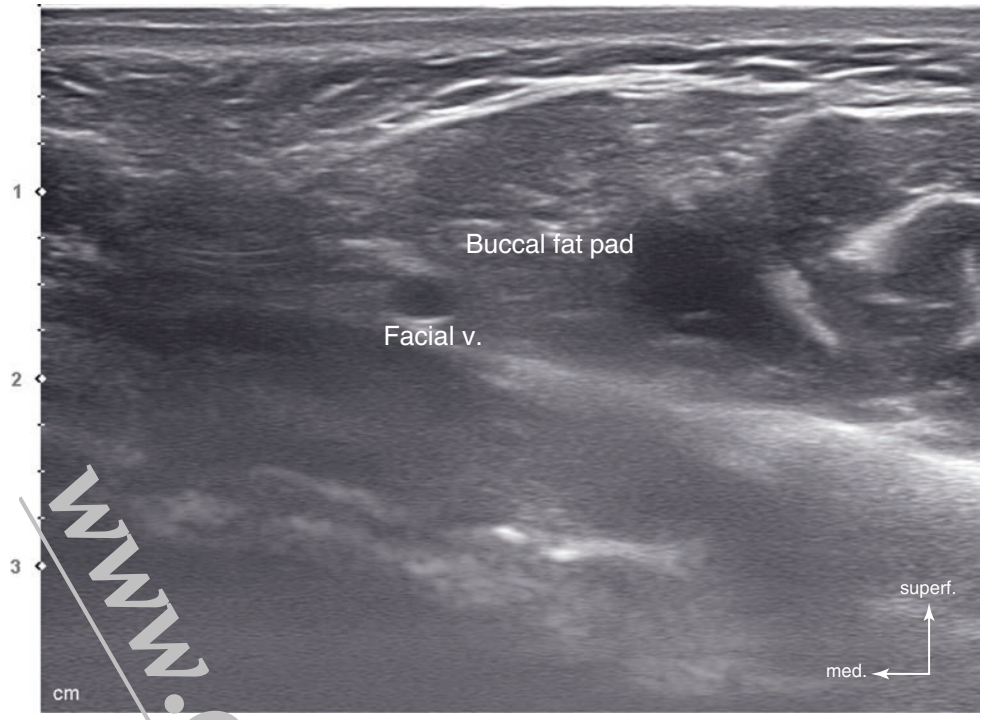

Fig. 2.17 Ultrasonography representing buccal fat pad (transverse view, 15 MHz by linear transducer). (Published with kind permission of © Hee-Jin Kim 2020. All Rights Reserved)

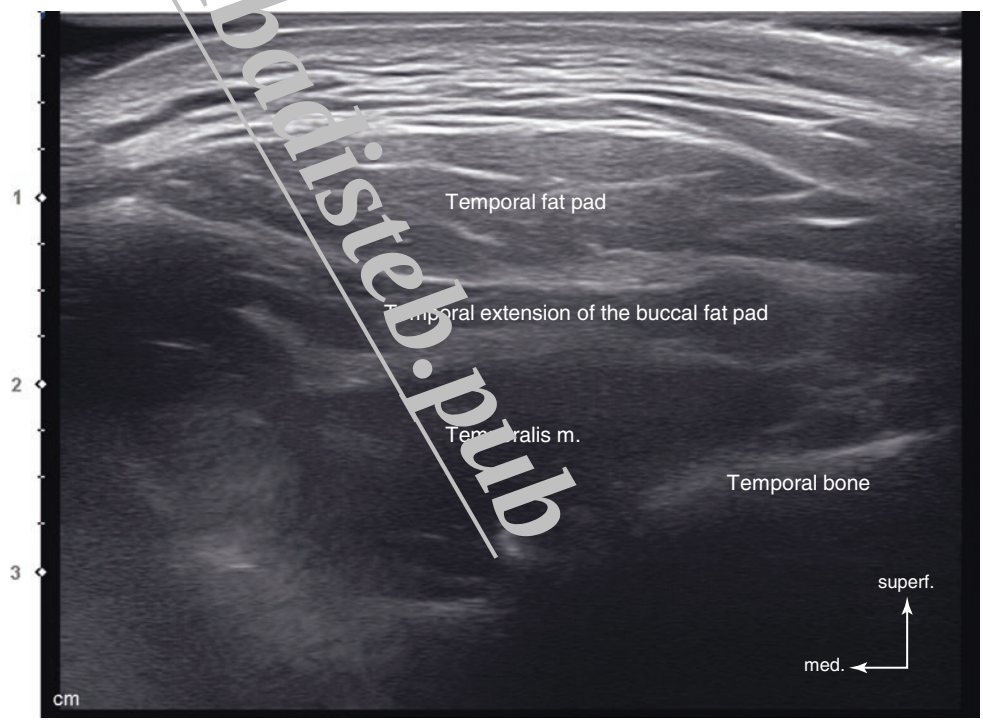

Fig. 2.18 Variable hypoechogenecity depending on the fat compartments of the temple. (Published with kind permission of © Hee-Jin Kim 2020. All Rights Reserved)

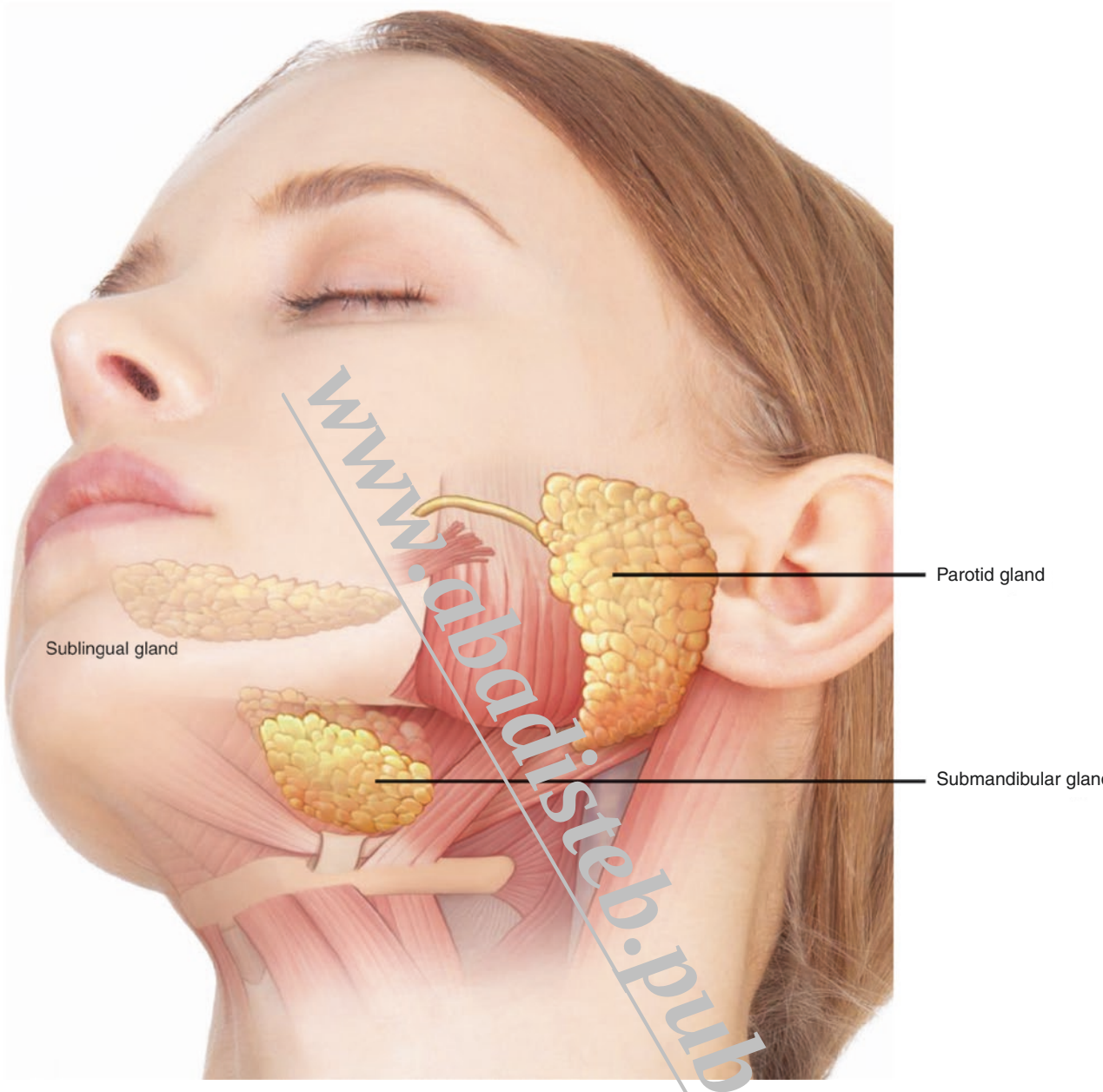

Fig. 2.19 Illustration of three major salivary glands. (Published with kind permission of © Kwan-Hyun Youn 2020. All Rights Reserved)

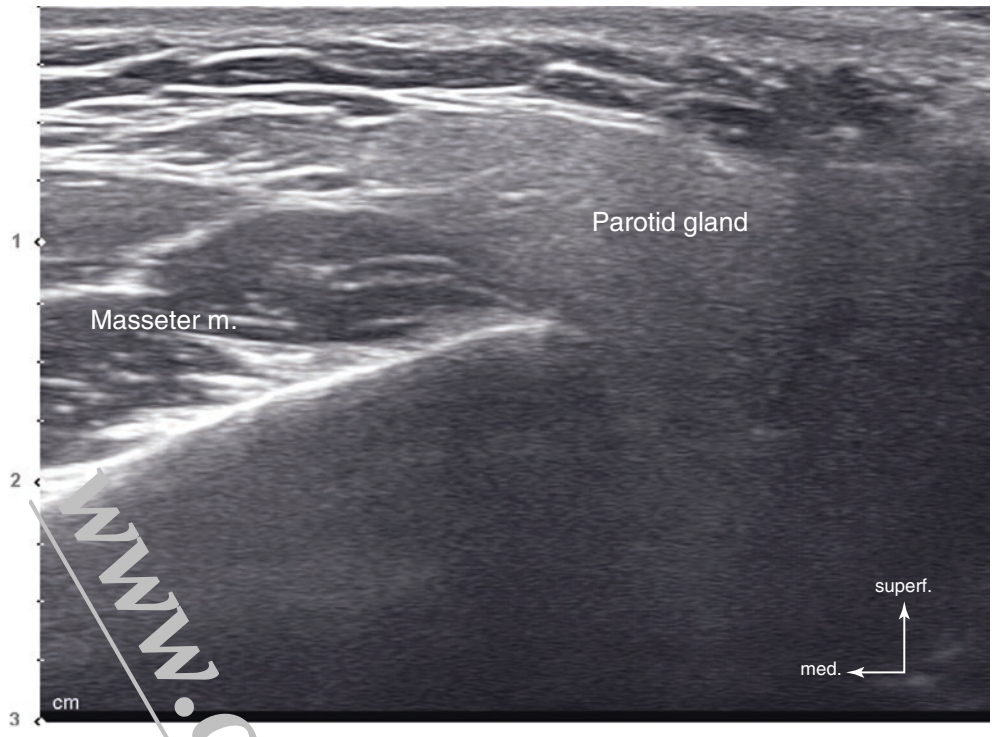

Fig. 2.20 Ultrasonography of the parotid gland (transverse view, 15 MHz by linear transducer). (Published with kind permission of © Hee-Jin Kim 2020. All Rights Reserved)

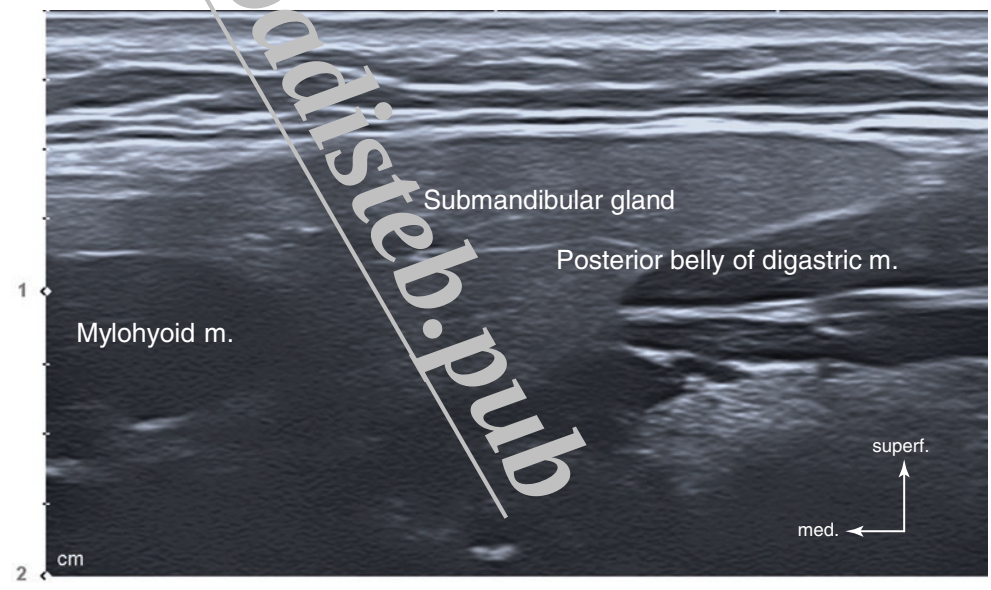

Fig. 2.21 Ultrasonography of the submandibular gland (transverse view, 15 MHz by linear transducer). (Published with kind permission of © Hee-Jin Kim 2020. All Rights Reserved)

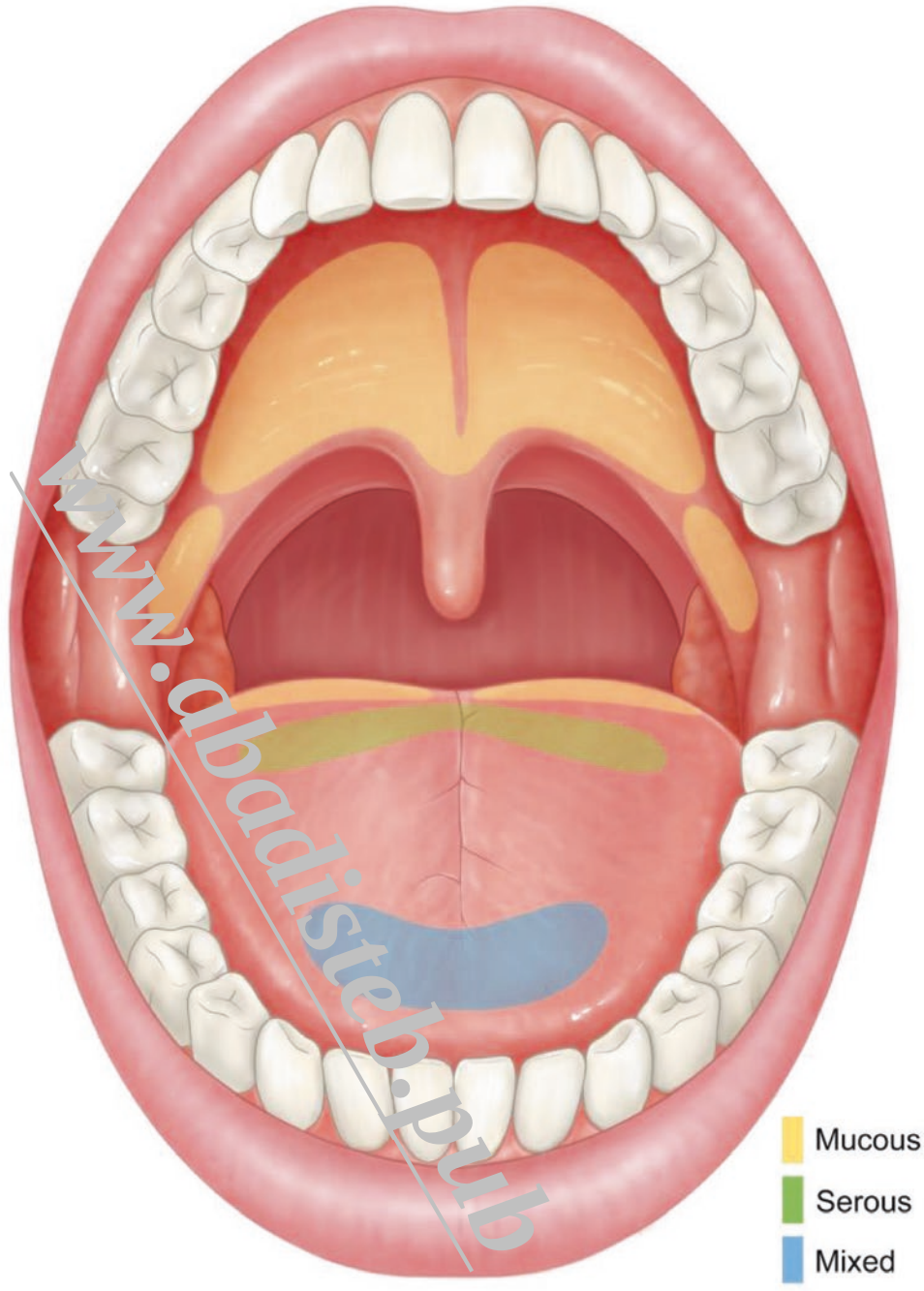

Fig. 2.22 Illustration of the locations and components of the minor salivary glands. (Published with kind permission of © Kwan-Hyun Youn 2020. All Rights Reserved)

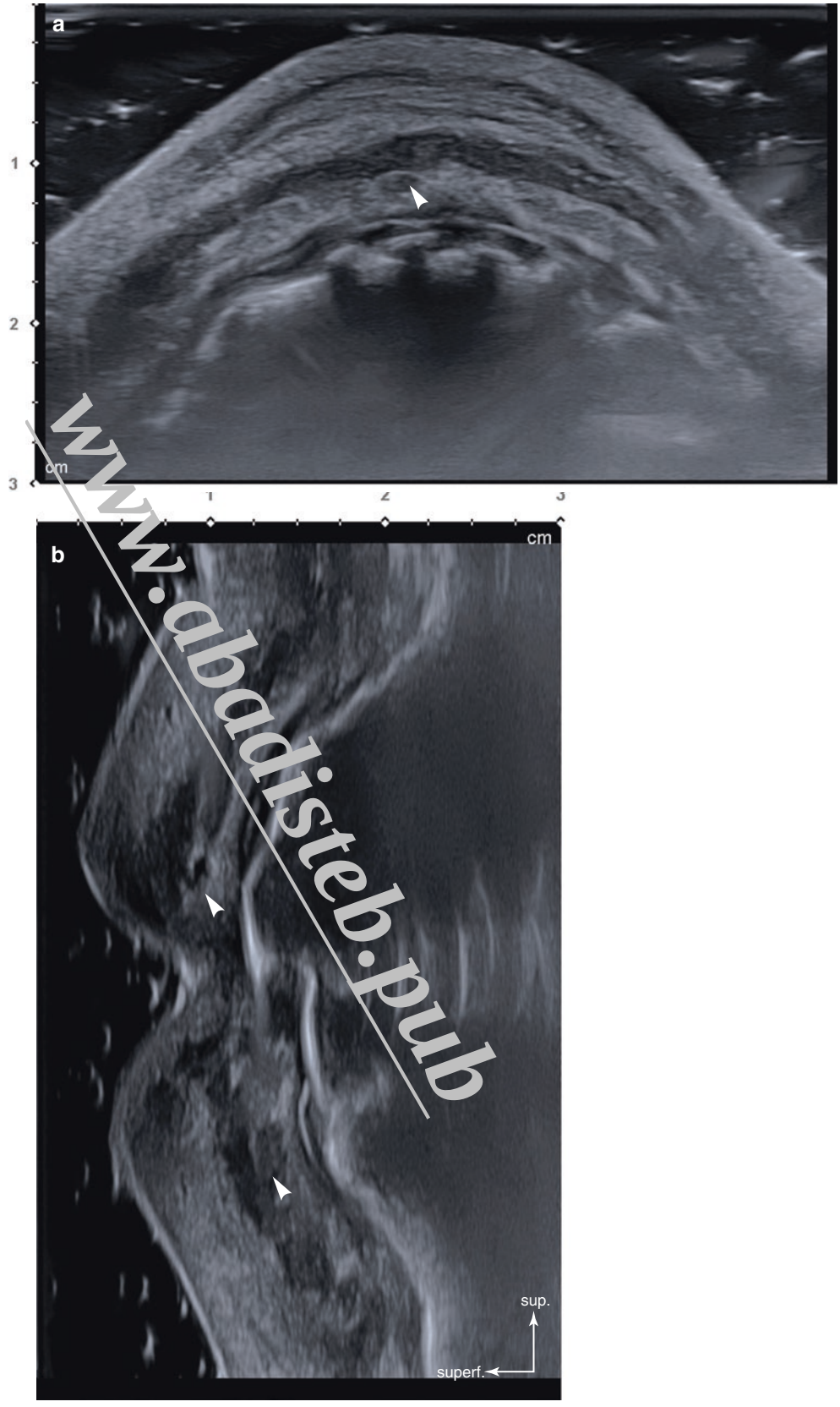

Fig. 2.23 Ultrasonography representing the minor salivary glands (arrowheads) of the lip. (**a**) Transverse view, 15 MHz by linear transducer and (**b**) sagittal view, 15 MHz by linear transducer. (Published with kind permission of © Hee-Jin Kim 2020. All Rights Reserved)

2.3 US Images of the Musculoskeletal Structures and Fasciae of the Face and Neck

The cortex of the bone appears as a hyperechoic line with posterior acoustic shadowing artifacts (Fig. 2.24).

The cartilage appears in US as hypoechoic bands, usually without detectable vascularity. These anatomical characteristics are seen in the nasal cartilages (upper and lower alar) and the ear cartilage (Fig. 2.25).

The muscles appear hypoechoic with muscle fibers and intramuscular tendinous structures showing dynamic changes under contraction and rest (Fig. 2.26). The tendons appear as hyperechoic structures with a fibrillary network, which are formed by parallel bundles of collagen (Fig. 2.27).

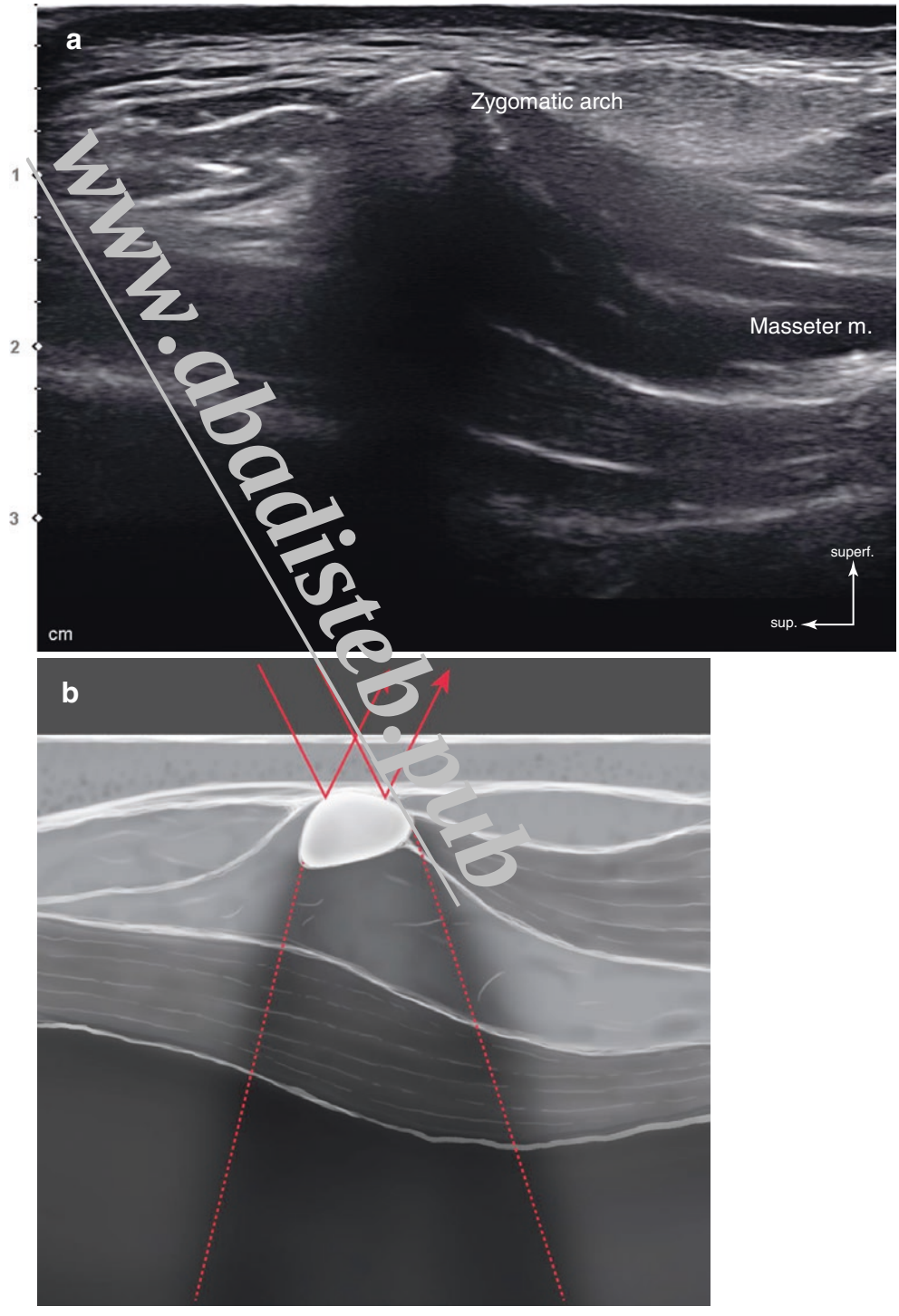

Fig. 2.24 Ultrasonography of bone and muscle. (**a**) Zygomatic arch (coronal view, 15 MHz by linear transducer) and (**b**) illustration representing phenomenon of the posterior acoustic shadowing. (Published with kind permission of © Hee-Jin Kim and Kwan-Hyun Youn 2020. All Rights Reserved)